

inter.noise 2000

*The 29th International Congress and Exhibition on Noise Control Engineering
27-30 August 2000, Nice, FRANCE*

I-INCE Classification: 3.1

NUMERICAL AND EXPERIMENTAL STUDY ON THE PERFORMANCE OF NOISE BARRIERS WITH A VARIETY OF SHAPES

S. Sakamoto, H. Tachibana

Institute of Industrial Science, University of Tokyo, 4-6-1 Komaba, Meguro-ku, 153-0041, Tokyo, Japan

Email: sakamo@cc.iis.u-tokyo.ac.jp

Keywords:

BARRIER, SECTION SHAPE, BEM, DIFFRACTION

ABSTRACT

The Maekawa's chart is often applied to the assessment of noise attenuation performances of barriers with various shapes and thickness. However, the applicability of this chart to such barriers with complicated shapes is not fully examined. As a basic investigation for the establishment of practical method to estimate the effect of noise barriers with various section shapes, numerical studies by 2-dimensional BEM and scale model experiment were performed.

1 - INTRODUCTION

For the reduction of such environmental noises as road traffic noise and railway noise, various counter-measures using noise barriers and design of road structures are applied. In order to assess their diffraction performances, the chart proposed by Maekawa [1] is widely being used. Although this chart is based on the simple Fresnel number concept for a single hemi-infinite barrier, it is often applied to more complicated barriers than a straight barrier. The applicability of this chart when extended to such barriers with a variety of section shapes is not fully examined. In this study, the effects of noise barriers with several shapes or thickness are investigated by 2-dimensional BEM and scale model experiment.

2 - CALCULATION METHOD

In a 2-dimensional sound field, the sound pressure at a point P is expressed as the following Helmholtz-Kirchhoff integral equation.

$$p(P) = p_s(P) + \int_S \left\{ p(Q) \frac{\partial G(P, Q)}{\partial n_Q} - \frac{\partial p(Q)}{\partial n_Q} G(P, Q) \right\} ds_Q \quad (1)$$

where $p(P)$ is the sound pressure, $p_s(P)$ is the sound pressure of the direct sound from the source, $G(P, Q)$ is the Green function (in 2-D sound field, $G(P, Q) = (1/4j) H_0^{(1)}(kr_{PQ})$, where $H_0^{(1)}(x)$ is the Hankel function of 0-order). When the barrier has thickness, Eq. (1) is applied for the calculation of the sound field.

In a special case of a rigid panel whose thickness becomes infinitely small, the sound pressure at the point P can be calculated using the following derivative forms of integral equation.

$$p(P) = p_s(P) + \int_S \tilde{p}(Q) \frac{\partial G(P, Q)}{\partial n_Q} ds_Q \quad (\text{for P in the external domain}) \quad (2)$$

$$-\frac{\partial p_s(P)}{\partial n_P} = \int_S \tilde{p}(Q) \frac{\partial^2 G(P, Q)}{\partial n_P \partial n_Q} ds_Q \quad (\text{for P on the boundary}) \quad (3)$$

where $\tilde{p}(Q)$ is the sound pressure difference between both sides of the panel at the point Q.

In cases where the thickness of the barrier is small, the sound field can be calculated by the Eqs. (2) and (3).

3 - NUMERICAL ANALYSIS AND EXPERIMENT

The sound attenuation performances of noise barriers with several shapes shown in figure 1 were investigated. In order to examine the differences of sound attenuation effects due to barrier shapes, these heights were equally assumed to be 5 m. As a boundary condition, the surfaces of the ground and the barriers assumed to be perfectly reflective. For the types 0, 1-a, 1-b and 1-c, Eqs. (2) and (3) were applied. The types 2 and 3 were calculated using Eq. (1).

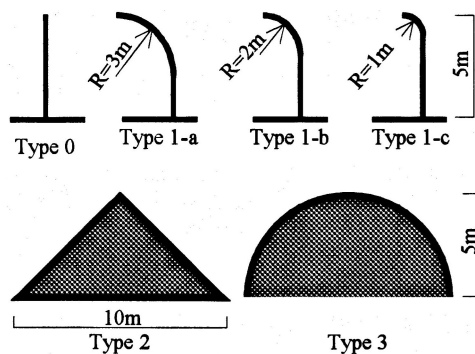


Figure 1: Barrier shapes under investigation.

3.1 - Comparison between calculation and experiment

In order to see the validity of the calculation, 1/20 scale model experiment was performed for the types 0, 1-a and 2. Figure 2 shows the scale model used in the experiment. This model has a 2-dimensional sound field with thickness of 10 mm. The cut-off frequency is around 17 kHz (850 Hz in real frequency). As a small omni-directional sound source, a spark discharge impulse source was attached on a rectangular acrylic pipe that corresponds to a ground. Under the experimental condition mentioned above, the sound pressure at the receiving point was measured for both cases of with and without barriers. The insertion loss was obtained as the difference of the squared and integrated sound pressure (sound energy). Comparisons between experimental and calculated results are shown in Fig. 3, in which it can be seen that the calculated and experimental results are fairly in good agreement.

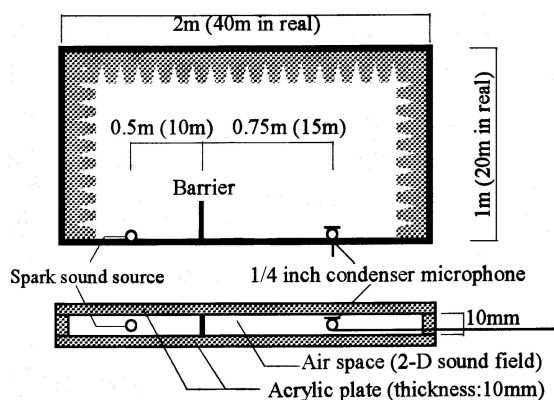


Figure 2: Experimental set up of 1/20 scale model.

3.2 - Numerical analysis

Calculated results by the BEM for the receiving points set at every 5 m from the barriers (see Fig. 4) are shown in Fig. 5. In cases of type 1-a, 1-b and 1-c, the sound attenuation effect is higher than that of the straight barrier (type 0). On the other hand, in cases of barriers with large thickness (types 2 and 3), the effects are much lower. Figure 6 shows the relationship between the Fresnel number and the sound attenuation effect for each case. In these figures, each dot indicates the value of sound attenuation calculated by the BEM and the curved lines show the attenuation levels calculated from the numerical expression of the Maekawa's chart [2]. The diffraction path length for the calculation of sound attenuation level using the Maekawa's chart was determined as shown in Fig. 7. In case of straight wall (type 0), the sound attenuation level agrees well with the calculated result from the Maekawa's chart. On the other

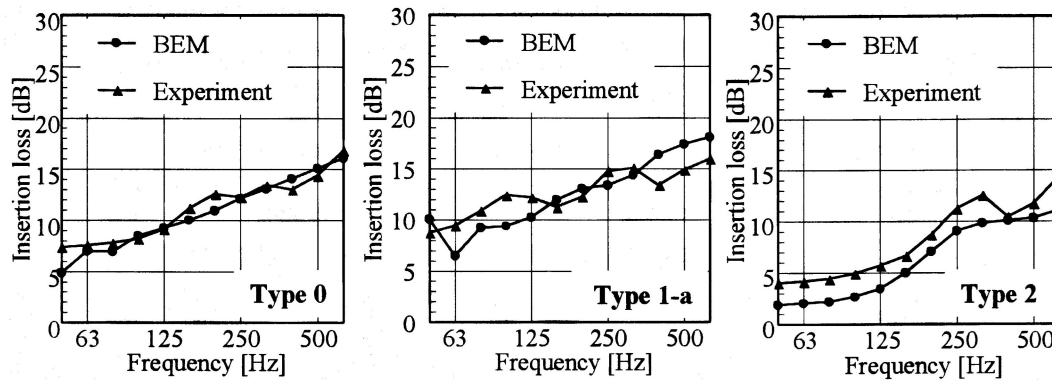


Figure 3: Comparison between BEM calculation and experimental results.

hand, for types 1-a, 1-b and 1-c, the sound attenuation level is about 3 dB higher than that obtained from the Maekawa's chart. This fact indicates that the Maekawa's chart tends to give underestimated reduction for barriers with such shapes. In cases of barriers with thickness (type 2 and 3), the reduction effect is 1 to 4 dB lower than the value obtained from the Maekawa's chart.

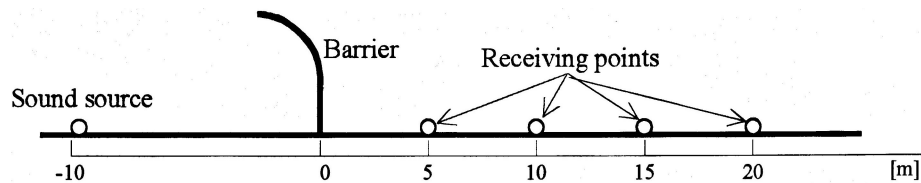


Figure 4: Geometrical condition of barrier, source and receiving points for numerical study.

4 - CONCLUSIONS

In this study, sound attenuation performances of noise barriers with several kinds of shapes were examined by numerical analysis using 2-dimensional BEM. From their results, the following facts have been found.

1. In case of straight barriers, the Maekawa's chart gives correct value of noise reduction as is well known.
2. On the other hand, in case where the tip part of the barrier is inclined inward as is often used for the reduction of road traffic noise lately, several dB higher reduction can be expected than that obtained by applying the Maekawa's chart.
3. On the contrary, in case of barriers with large thickness, the reduction is lower than that obtained by applying the Maekawa's chart.

Such tendencies must be carefully noted for the design of noise barriers with such shapes and thickness as dealt in this study.

REFERENCES

1. **Z. Maekawa**, Noise reduction by screens, *Applied Acoustics*, Vol. 1, pp. 157-173, 1968
2. **K. Yamamoto and K. Takagi**, Expressions of Maekawa's chart for computation, *Applied Acoustics*, Vol. 37, pp. 75-82, 1992

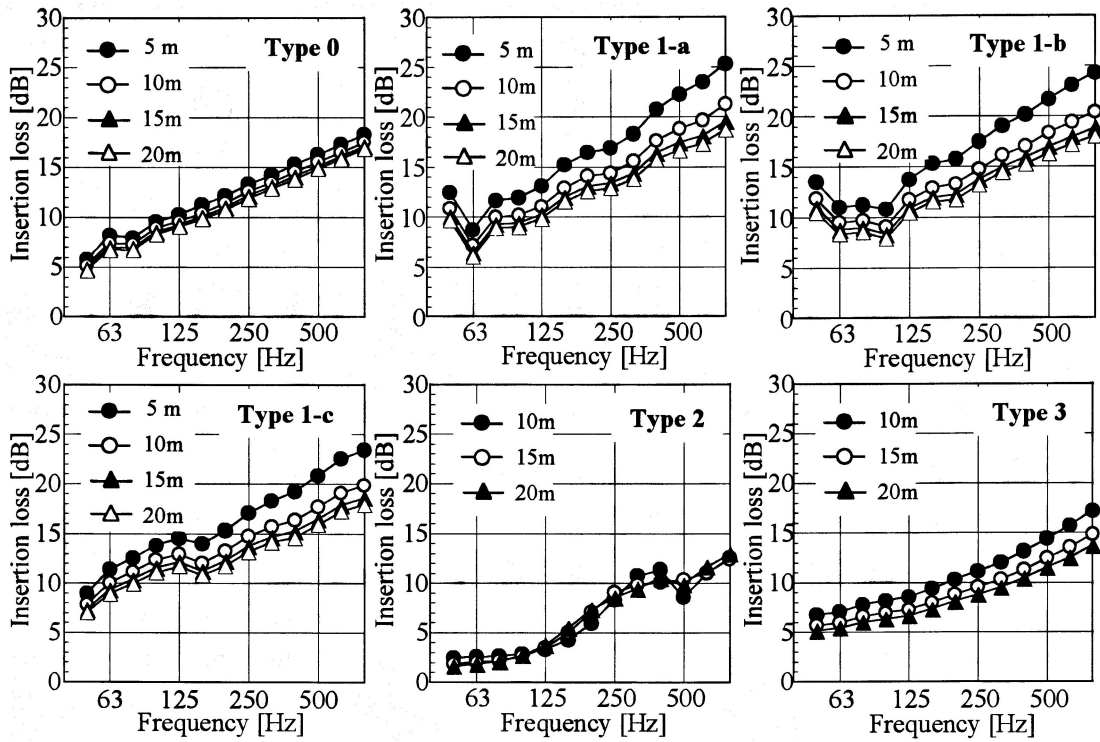


Figure 5: Insertion loss of noise barriers.

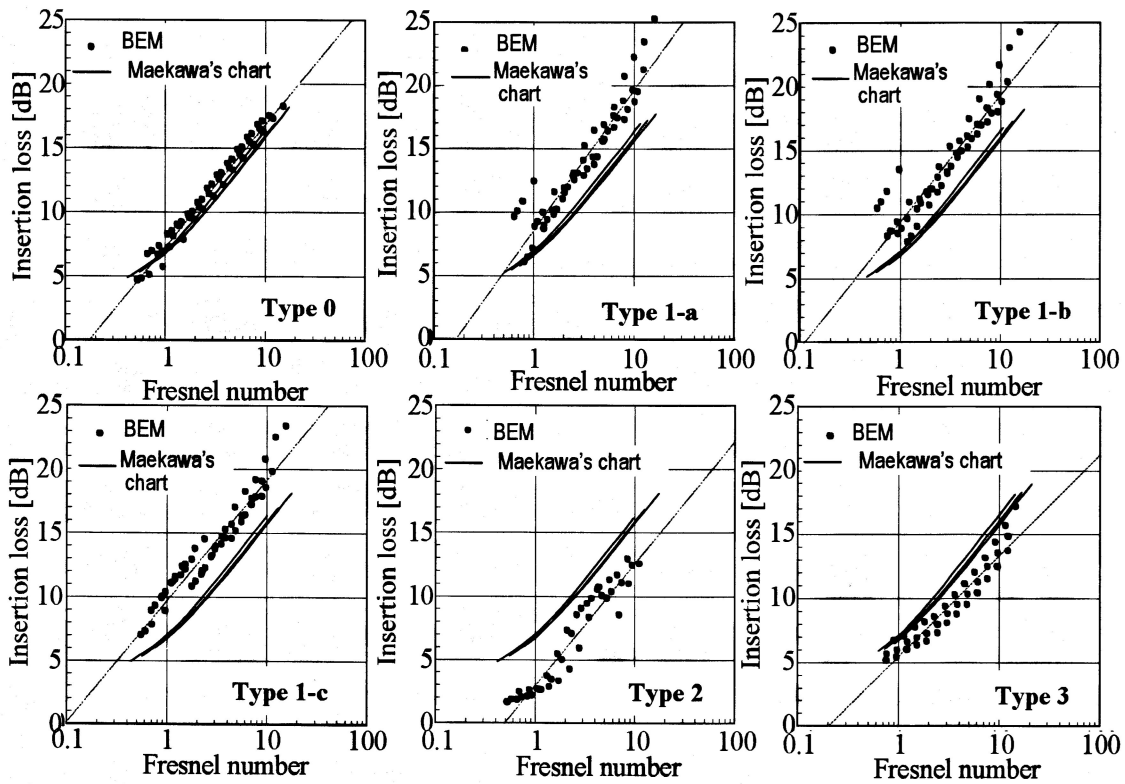


Figure 6: Relationship between Fresnel number and sound attenuation effects.

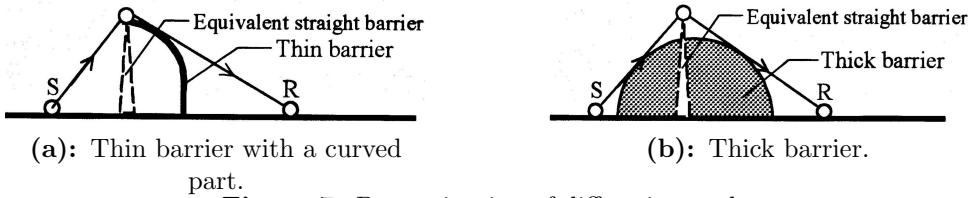


Figure 7: Determination of diffraction path.